

RSC Advances



This is an *Accepted Manuscript*, which has been through the Royal Society of Chemistry peer review process and has been accepted for publication.

Accepted Manuscripts are published online shortly after acceptance, before technical editing, formatting and proof reading. Using this free service, authors can make their results available to the community, in citable form, before we publish the edited article. This *Accepted Manuscript* will be replaced by the edited, formatted and paginated article as soon as this is available.

You can find more information about *Accepted Manuscripts* in the [Information for Authors](#).

Please note that technical editing may introduce minor changes to the text and/or graphics, which may alter content. The journal's standard [Terms & Conditions](#) and the [Ethical guidelines](#) still apply. In no event shall the Royal Society of Chemistry be held responsible for any errors or omissions in this *Accepted Manuscript* or any consequences arising from the use of any information it contains.



Journal Name

COMMUNICATION

Nanocomposite preparation *via in-situ* polymerization of quaternary ammonium salt ion-bonded to graphite platelets

Received 00th January 20xx,
Accepted 00th January 20xx

L. Poláková,^{†a} H. Beneš,^a P. Ecorchard,^b E. Pavlová,^a Z. Sedláková,^a J. Kredatusová^a and V. Štengl^b

DOI: 10.1039/x0xx00000x

www.rsc.org/

Here we report a novel method of intercalation of quaternary ammonium salt bearing polymerizable group in between graphite galleries. By the exfoliation of the intercalate during its subsequent polymerization with *n*-butyl methacrylate, polymer membrane with homogeneously dispersed graphene nanostructures was obtained.

Preparation and characterization of graphite intercalation compounds (GICs) using low-molecular weight quaternary ammonium salts as well as exfoliation of GIC for preparation of single or few layered graphene nanosheets have been intensively studied by many authors. Tetraalkylammonium (TAA) cations as graphite delaminating agents prepared by electrochemical reduction in a suitable solvent were successfully applied for preparation of GICs.¹⁻³ Recently, Sirisaksoontorn et al. have developed a smart method of intercalation of TAA cations *via* rapid ion-exchange reaction with sodium-ethylenediamine cation ([Na(en)]⁺) complex within graphite galleries.^{4,5}

Despite the large amount of the synthesized GICs, only a few have been directly applied for *in-situ* polymerization and preparation of graphite/polymer nanocomposites, since organic molecules are hard to be directly intercalated into the space between graphite sheets. Xiao et al. reported *in-situ* polymerization of styrene in a ternary K-THF-GIC solution system.⁶ However, simple "swelling" of GIC in the monomer does not ensure that the polymerization takes place in the graphite interlayers. *In-situ* polymerization with initiator-intercalated graphite was described by several authors.⁷⁻⁹ Shioyama showed that GIC of alkali metals formed ternary compounds initiating the polymerization in the interlayer spacing of graphite if unsaturated hydrocarbons were co-intercalated.¹⁰ All the above mentioned approaches are aimed

to gain homogeneous dispersions of exfoliated graphite-based nanoplatelets in the polymer matrix. Advanced nanocomposites with improved electrical and thermal properties,^{11,12} increased mechanical strength^{13,14} or gas-selective barrier properties¹⁵ can thus be prepared. In our previous studies, polymers with homogeneously dispersed exfoliated clay nanoplatelets were prepared where (meth)acrylate monomers containing ammonium group were intercalated into inorganic layered hosts.¹⁶⁻¹⁸

Here we first report a smart method for preparation of polymer membrane with dispersed graphene structures, which consists in intercalation of ([Na(en)]⁺) complex into the graphite galleries, followed by ion-exchange reaction of the complex with quaternary ammonium salt bearing polymerizable methacrylamide group, and as a last step an exfoliation process during polymerization of the prepared GIC with *n*-butyl methacrylate.

To our best knowledge, this synthetic strategy for preparation of graphene structures containing nanocomposite polymer membranes has not yet been published. Contrary to other known techniques, one of the main advantages of our present route consists in the presence of polymerizable groups attached by ionic interactions to the graphite platelets, ensuring that the polymerization takes place inside the galleries thus enhancing the exfoliation process.

Quaternary salt (DM16) was prepared by reaction of *N*-[3-(dimethylamino)propyl] methacrylamide (DMAPMA) with *n*-hexadecyl iodide. Our attempts of a direct intercalation of this ammonium salt into graphite galleries by a simple reaction of DM16 with pristine graphite were not successful. Therefore, GIC intercalated by [Na(en)]⁺ complex was synthesized first (GIC G1).⁴⁻⁵ A redox process during the reaction of sodium metal with ethylenediamine (en) enhances the intercalation of the forming complex in between the graphene sheets. Subsequently, an ion-exchange reaction of the incorporated cation complex with the DM16 monomer was successfully carried out (GIC G2). The polymer composites of polyBuMA with pristine graphite, G1 and G2 (PG, PG1 and PG2, respectively) were synthesized by free radical polymerization

^a Institute of Macromolecular Chemistry, AS CR v.v.i., Heyrovsky Sq. 2, 162 06 Prague 6, Czech Republic.

^b Institute of Inorganic Chemistry, AS CR v.v.i., 250 68 Řež, Czech Republic.

[†] corresponding author. E-mail: polakova@imc.cas.cz

Electronic Supplementary Information (ESI) available: Materials, methods of measurements, synthetic procedures, Fig. S1-S5, Table S1. See DOI: 10.1039/x0xx00000x

in DMSO. This solvent was used to ensure a uniform dispersion of the synthesized GICs at the beginning of polymerization. Details of all the synthetic procedures can be found in ESI. For better illustration, the scheme of the synthetic route leading to polymer nanocomposite is depicted in Fig. 1.

The prepared GICs were characterized using TGA-FTIR (Fig. 2). The TG curve of pure graphite did not show any significant weight loss till 700 °C (Fig. 2a). The G1 intercalate showed a two-step mass loss (total 20 wt.%) at 50–400 °C (Fig. 2b). The FTIR spectra of gases released in this temperature region during TGA of G1 and of en are shown in Fig. 3a. Evidently, en is present to some extent in the G1 intercalate: peaks at 3310–3450 cm^{-1} (N–H stretching), 772 cm^{-1} (N–H wagging), 1620 cm^{-1} (–NH₂ bending), 2770–3025 cm^{-1} (C–H stretching), 1472 cm^{-1} and 1363 cm^{-1} (–CH₂ bending and wagging, respectively), and 1046 cm^{-1} (skeletal vibration).^{19,20} This is in accordance with Sirikasoontorn et al., who suggested direct intercalation of the sodium-en complex within the graphene sheets.⁴

The first weight loss (8 wt.%) of G2 intercalate at 60–145 °C (Fig. 2c) was attributed to the volatilization of en, which was also confirmed by FTIR analysis of the evolved gases (Fig. S1). Apparently, [Na(en)]⁺ complex was not completely displaced by DM16 monomer from the GIC galleries. The second weight loss (7 wt.%) at 150–260 °C was assigned to both the volatilization of en and the degradation of intercalated DM16 monomer. The latter was more obvious from the FTIR spectra of evolved gases during TGA at higher temperatures (Fig. S1), when a multistep weight loss (22 wt.% in total at region of 275–700 °C) attributed mainly to the decomposition of intercalated DM16 monomer took place (Fig. 2c). The slow mass decrease at the last stage of thermal degradation (above ca 600 °C) was assigned to the evolution of products due to both pyrolytic degradation of the intercalated DM16 monomer and loss of graphitic carbon mass, oxidatively damaged during the GIC synthesis. However, the observed minor extent of the latter is expected since mild synthetic conditions were applied. The TG curve of DM16 exhibited main weight loss at 120–400 °C, when the majority of the sample (99 wt.%) decomposed (Fig. 2d). The slow mass loss above 400 °C was accompanied by evolution of gaseous pyrolytic products (Fig. S2). To support the TGA-FTIR results, G2 intercalate was further analyzed using ATR-FTIR spectroscopy.

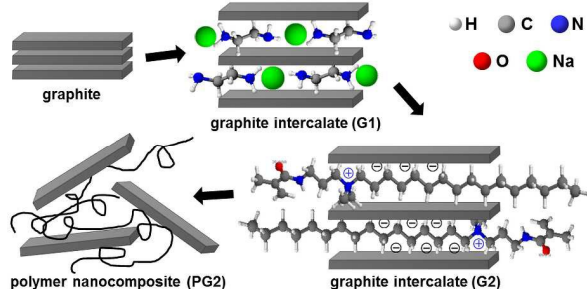
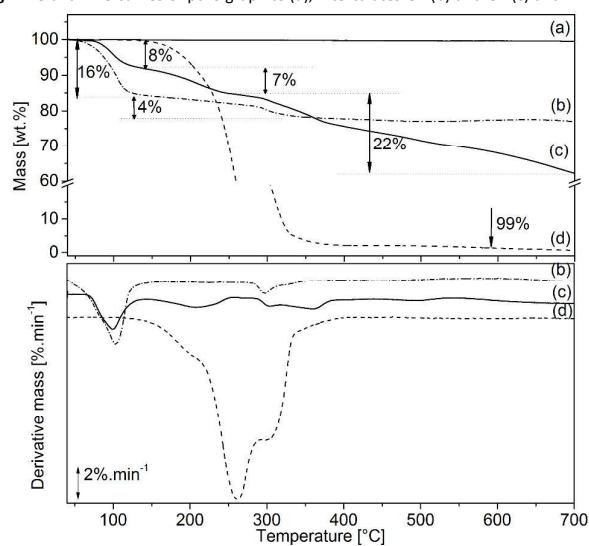


Fig. 1 Scheme of the polymer nanocomposite (PG2) preparation.

Fig. 2 TG and DTG curves of pure graphite (a), intercalates G1 (b) and G2 (c) and DM16



monomer (d).

Contrary to the absorbance spectrum of natural graphite (not shown here), which was featureless in the fingerprint region, the spectrum of G2 displayed absorptions probably originating from both DM16 and the [Na(en)]⁺ complex. To subtract the absorptions coming from the latter, differential spectrum of G2 referenced to G1 was compared to the spectra of pure en and DM16 (Fig. 3b). The highlighted peaks indicate the presence of intercalated DM16 monomer: the peaks at 3350 cm^{-1} and 1545 cm^{-1} (stretching and bending vibrations, respectively, of N–H amide group), 3015 cm^{-1} (stretching of C–H alkene group), and 1646 cm^{-1} (stretching of amide C=O).²¹

XRD technique was employed in order to determine the structure of the prepared intercalates with emphasis on changes in layer arrangement. The structure of graphite involves mutually parallel graphene layers with (002) reflection at $2\theta = 26.4^\circ$ (Fig. 4a) and the basal repeat distance of 0.337 nm. This value is commonly regarded as the interplanar spacing and corresponds to the van der Waals diameter of carbon atom.²² The reaction of graphite with sodium metal in the presence of en yielded ordered first-stage GIC G1 with significantly larger basal spacing (0.693 nm, $2\theta = 12.8^\circ$).

The gallery expansion is a consequence of the intercalation of the formed [Na(en)]⁺ complex (in parallel orientation²³) in between the single graphene layers.^{4,5} After the ion-exchange reaction of the DM16 quaternary salt with the [Na(en)]⁺ complex, the resulting first-stage intercalate G2 exhibited (001) reflection corresponding to a basal repeat distance of 0.697 nm ($2\theta = 12.7^\circ$), giving interlayer spacing of 0.360 nm. Clearly, the gallery height is given by the size of the intercalated cation.

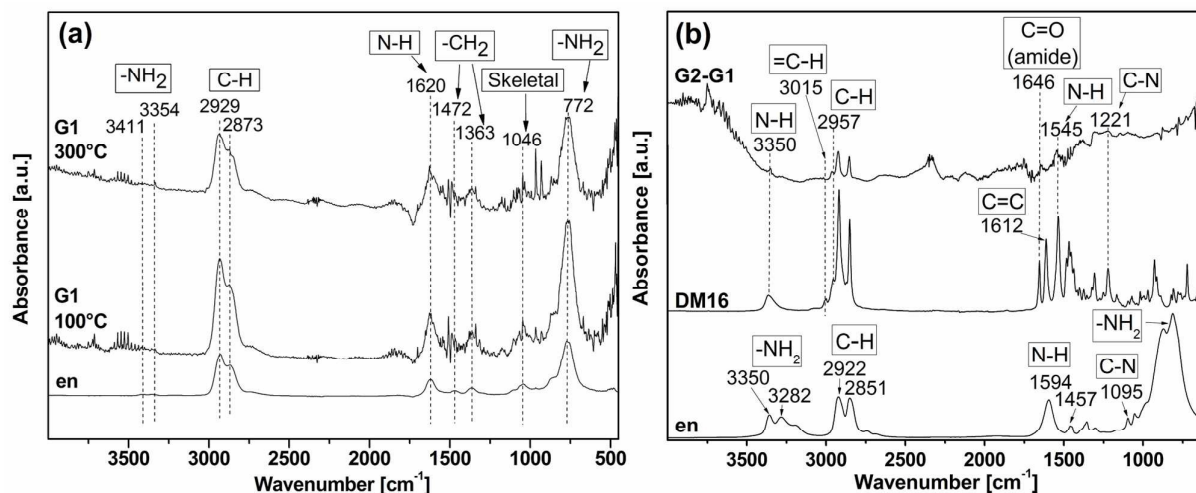


Fig. 3 (a) FTIR spectra of the gases released during TGA of en and G1 intercalate during the mass loss at 100 °C and at 300 °C. (b) FTIR spectra of en, DM16 monomer, and the differential spectrum of G2 intercalate referenced to the spectrum of G1 intercalate (G2-G1).

The interlayer spacing of 0.360 nm is in a good agreement with the predicted thickness (0.359 nm) of the layer containing the DM16 ammonium salt in the fully tetrahedral conformation with aliphatic chains oriented parallel to the graphene sheets. This value was determined using ACD/ChemSketch software for 3D imaging; data used for calculation are presented in the ESI (Tab. S1).

SEM photographs of the GICs are shown in Fig. 4b. Pristine graphite flakes exhibit a layered structure with densely packed

nanosheets.¹⁴ The layered morphology was maintained after chemical modification of the graphite. Samples G1 and G2 consist of intercalated stacks, rippled sheets with curved edges, giving evidence that the modification of graphite was successful in both GICs.⁴

The polymer composites were prepared in the form of polymer membranes with thickness of ca 200 μm using solution casting technique from THF (Fig. 4c).

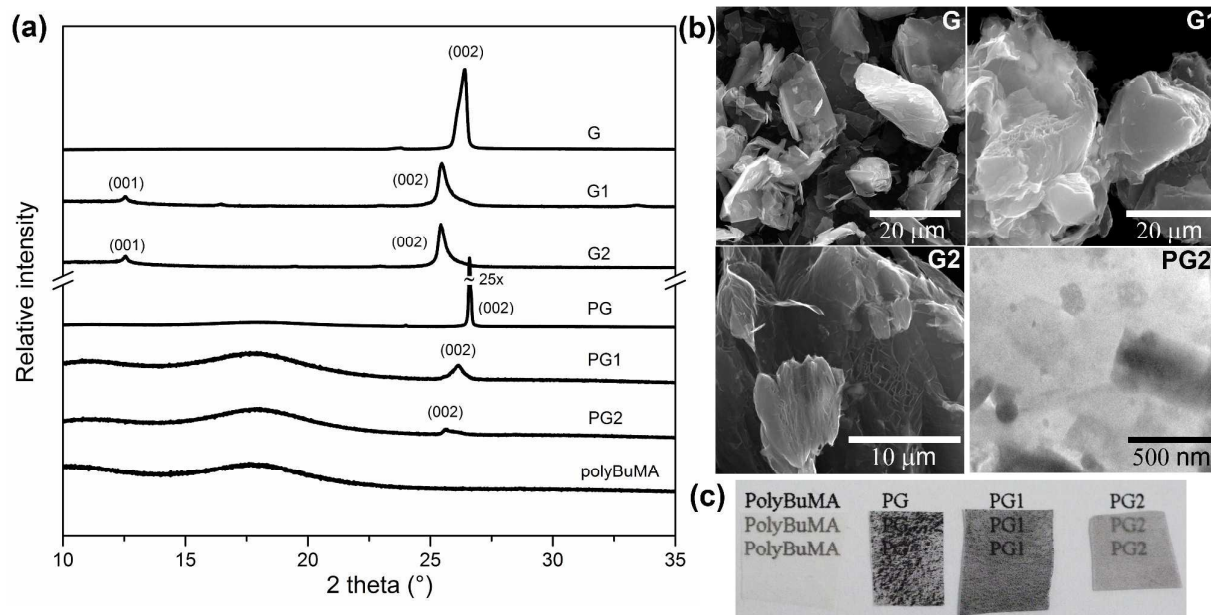


Fig. 4 (a) XRD patterns of the graphite (G), G1 and G2 intercalates, PG, PG1 and PG2 polymer nanocomposites, and neat polyBuMA. (b) SEM images of the pristine graphite (G), G1 intercalate with stacked layer by layer structure, G2 intercalate with expanded and flattened honeycomb-like structure, and TEM image of the PG2 polymer nanocomposite. (c) Photos of polymer membranes (200 μm thick): neat polymer (polyBuMA) and polymer composites filled with 0.1 wt.% of natural graphite (PG), G1 intercalate (PG1) and G2 intercalate (PG2).

In-situ polymerization in the presence of pristine graphite led to a formation of large aggregates and heterogeneities in the resulting polyBuMA composite (PG). The usage of G1 intercalate allowed for better filler dispersion in the polymer matrix (PG1). However, a completely homogenous polymer composite without visible agglomerates was prepared when G2 intercalate was used as the filler (PG2 sample).

WAXS curves of all polyBuMA-containing samples exhibited three distinct maxima at low angles ($2\theta = 8.1^\circ$, 10.2° and 17.8°) corresponding to the structure of the polymer matrix.¹⁸ In comparison with neat graphite, visible narrowing of the (002) graphite reflection can be seen in the graphite-containing nanocomposite (PG). This effect could be attributed to an influence of the *in-situ* formed polyBuMA matrix on the stacking of unmodified graphene layers in the graphite sample. Upon polymerization no (001) reflections at $2\theta = 12.8^\circ$ and 12.7° were observed in the polymer nanocomposites PG1 and PG2, respectively, indicating that graphene platelets were formed and dispersed in the polymer matrix.¹⁶⁻¹⁸ Interestingly, a new maximum in PG1 nanocomposite appeared at $2\theta \sim 26.2^\circ$ (0.340 nm), which corresponds to the initial position of the high-angle shoulder of (002) reflection in the neat G1 intercalate. This suggests that a weakly modified graphite is present to a certain small extent in the starting G1 intercalate. Consequently, the presence of the small amount of this high-stage intercalate remaining un-exfoliated in the PG1 nanocomposite is observable as a distinct diffraction maximum. On the other hand, the shape and position of the (002) reflection of the PG2 composite corresponds to G2 intercalate, indicating the absence of poorly modified high-stage intercalate in the PG2 composite. Moreover, significant differences in the shape and position of the (002) reflection can be seen between PG and PG2 polymer composites, giving evidence that only a negligible amount of the un-exfoliated part of the highly ordered G2 intercalate was found in the PG2 nanocomposite. It is known that WAXS results by themselves could not be used as a self-standing description of nanocomposite structure at low filler loadings. Therefore, additional TEM investigation was done.

In the TEM image of the PG2 polymer nanocomposite (Fig. 4b), graphene nanosheets can be observed, partially supplemented with few-layered structures with higher packing densities, which is in agreement with WAXS results. To obtain more detailed information about the filler dispersion, the STEM method was also employed (Fig. S3). Here, the results show that in the PG composite the size of graphitic particles remained almost unchanged after polymerization (Fig. S3a). On the other hand, the much thinner, smaller and homogeneously dispersed particles can be observed in the PG2 composite, giving evidence that the intercalation/exfoliation process proceeded successfully (Fig. S3b). To further support the idea that the quaternary salt plays an important role during the exfoliation process, another experiment was conducted where a new GIC (G3) was synthesized by an exchange reaction between the G1 intercalate and neat *n*-hexadecyl iodide. Subsequently, the

resulting GIC was used in the preparation of polyBuMA composite under similar conditions as for PG1 and PG2 samples (see ESI). However, large macroscopic agglomerates of graphitic particles were observed in the prepared PG3 membrane (Fig. S4a). Furthermore, SEM and STEM images (Fig. S4b-c) of PG3 showed a tendency of the micrometric G3 filler to pull out of the polymer matrix thus indicating poor compatibility of this filler with polyBuMA. In contrast, even the larger flakes of G2 intercalate ionically bound to the polymer chain exhibited much better compatibility with polyBuMA in which they were homogeneously dispersed (Fig. 4b and S3).

The PG2 nanocomposite containing 0.0375 wt.% of graphite/graphene exhibited the value of coefficient of thermal conductivity (λ) equal to the PG composite loaded with ca 3 times higher amount of untreated graphite filler (Table 1). The significant increase of λ (of 62 % above the original polyBuMA value) was reached when the content of the filler in PG2 was doubled to 0.075 wt.%. Homogeneous filler distribution and its exfoliated structure in the PG2 composites led to an increased contact surface area between the filler and the polyBuMA, resulting in increased thermal conductivity due to decreasing interfacial thermal resistance.^{24,25} The measured values of specific heat capacity (c_p) are in a good accordance with the measured λ values; i.e. more conductive materials exhibited lower values of c_p . Thermal stability of the prepared nanocomposites determined by TGA correlated well with the filler content and was significantly improved in all samples (expressed as $T_{5\%}$ and $T_{10\%}$ values) in comparison to the neat polymer matrix.

The PG2 nanocomposites with higher loadings of G2 (0.25 wt.% and 0.5 wt.%) were also prepared to demonstrate the effect of nanofiller on mechanical properties (see Fig. S5). At rubber state, the addition of 0.5 wt.% G2 (i.e. the content of graphite/graphene filler of 0.38 wt.%) increased both Young's modulus (+27%) and tensile strength (+17%) confirming filler-polymer interactions²⁶, whereas the elongation at break and toughness decreased gradually. Similar mechanical improvement was reported by Chen et al.⁸ for the *in-situ* prepared GIC/polystyrene nanocomposites.

Table 1 Properties of neat polymer matrix (polyBuMA) and PG and PG2 polymer nanocomposites.

Sample	Filler conc. wt.%	c_p J/(g.K)	λ W/(m.K)	T_g °C	$T_{5\%}$ °C	$T_{10\%}$ °C
PolyBuMA	0	1.33	0.13	30	283	293
PG2	0.05* (0.0375)	1.23	0.17	31	293	307
PG2	0.1* (0.075)	1.20	0.21	33	300	309
PG	0.1	1.22	0.16	34	304	316

* Content of GIC. The total content of the graphite/graphene is given in brackets (determined from TGA).

c_p determined at glassy state at 10 °C (from DSC)

T_g – determined as a midpoint of modulated temperature (from DSC)

$T_{5\%}$, $T_{10\%}$ – the temperature of 5 % and 10 %, respectively, of the total sample mass loss (from TGA)

Conclusion

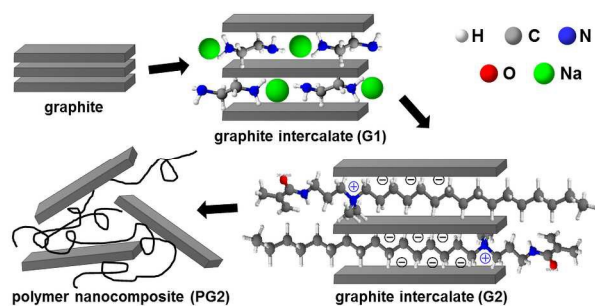
Methacrylamide monomer containing a covalently bonded quaternary ammonium group was synthesized and characterized. The prepared ammonium salt was successfully intercalated in between graphite platelets *via* ion-exchange reaction. Upon polymerization process of the intercalate with *n*-butyl methacrylate, polymer membrane with homogeneously dispersed exfoliated graphene nanoplatelets exhibiting significantly increased thermal conductivity and thermal stability was prepared. However, a certain amount of unexfoliated intercalate was still present in the composite. Therefore, our next and more detailed study will be focused on the optimization of reaction conditions of both intercalation and subsequent polymerization reactions in order to ensure the exfoliation process to a higher extent. Relationship between morphology and physical properties (gas permeability behavior as well as improved electrical properties) of the prepared nanocomposites will be also evaluated in details. The developed process has a broad application potential in the field of graphene-based polymer nanocomposites because of the low cost of graphite and the versatility of monomers used for the *in-situ* polymerization.

Acknowledgement

The authors are grateful to the Grant Agency of the Czech Republic (project 14-05146S) for financial support.

Notes and references

- J.O. Besenhard, H. Möhwald and J.J. Nickl, *Carbon*, 1980, **18**, 399.
- J. Simonet and H. Lund, *J. Electroanal. Chem.*, 1977, **75**, 719.
- M. Noel and R. Santhanam, *J. Power Sources*, 1995, **56**, 101.
- W. Sirisaksoontorn, A.A. Adenuga, V.T. Remcho and M.M. Lerner, *J. Am. Chem. Soc.*, 2011, **133**, 12436.
- W. Sirisaksoontorn and M.M. Lerner, *Inorg. Chem.*, 2013, **52**, 7139.
- M. Xiao, L. Sun, J. Liu, Y. Li and K. Gong, *Polymer*, 2002, **43**, 2245.
- G.H. Chen, D.J. Wu, W.G. Weng, B. He and W.L. Yan, *J. Appl. Polym. Sci.*, 2001, **82**, 2506.
- G.H. Chen, D.J. Wu, W.G. Weng, B. He and W.L. Yan, *Polym. Int.*, 2001, **50**, 980.
- G.H. Chen, W.G. Weng, D.J. Wu and W.L. Yan, *Polymer*, 2003, **44**, 1781.
- H. Shioyama, *J Mater. Chem.*, 2001, **11**, 3307.
- N. Park, J. Lee, H. Min, Y.D. Park and H.S. Lee, *Polymer*, 2014, **55**, 5088.
- G.D. Park, H.O. Jung, K.M. Kim, J.H. Lim, J.W. Lee, S.G. Lee, J.H. Lee and S.R. Kim, *Macromol. Res.*, 2015, **23**, 396.
- M. Fang, K. Wang, H. Lu, Y. Yang and S. Nutt, *J. Mater. Chem.*, 2009, **19**, 7098.
- M. Naebe, J. Wang, A. Amini, H. Khayyam, N. Hameed, I.H. Li, Y. Chen and B. Fox, *Sci. Rep.*, 2014, **4**, 4375.
- A.M. Pinto, J. Cabral, D.A.P. Tanaka, A.M. Mendes and F.D. Magalhães, *Polym. Int.*, 2013, **62**, 33.
- J.M. Herrera-Alonso, Z. Sedlakova and E. Marand, *J. Mem. Sci.*, 2010, **349**, 251.
- Z. Sedlakova, J. Pleštil, J. Baldrian, M. Šlouf and P. Holub, *Polym. Bull.*, 2009, **63**, 365.
- F. Kovanda, E. Jindova, K. Lang, P. Kubát and Z. Sedlakova, *Appl. Clay Sci.*, 2010, **48**, 260.
- Y.L. Lam and H.H. Huang, *J. Mol. Struct.*, 1997, **412**, 141.
- M.G. Giorgini, M.R. Pelletti, G. Paliani and R.S. Cataliotti, *J. Raman Spectrosc.*, 1983, **14**, 16.
- R.M. Silverstein, G.C. Bassler, T.C. Morrill, *Spectrometric identification of organic compounds*, 1991, John Wiley & Sons, Inc., 5th edition.
- R.R. Haering, *Can. J. Phys.*, 1958, **36**, 352.
- A.U. Liyanage and M.M. Lerner, *RSC Adv.*, 2014, **4**, 47121
- C.C. Teng, C.C.M. Ma, C.H. Lu, S.Y. Yang, S.H. Lee, M.C. Hsiao, M.Y. Yen, K.C. Chiou and T.M. Lee, *Carbon*, 2011, **49**, 5107
- M.C. Hsiao, C.C.M. Ma, J.C. Chiang, K.K. Ho, T.Y. Chou, X. Xie, C.H. Tsai, L.H. Chang and C.K. Hsieh, *Nanoscale*, 2013, **5**, 5863
- J.Y. Jang, M.S. Kim, H.M. Jeong and C.M. Shin, *Comp. Sci. Technol.*, 2009, **69**, 186



Polymerizable groups attached by ionic interactions to the graphite galleries ensure the polymerization takes place inside the galleries thus enhance the exfoliation process.